International Journal of Engineering Sciences & Emerging Technologies, Mar. 2015.
ISSN: 22316604 Volume 7, Issue 5, pp: 725-736 ©IJESET

DEPTH BASEMENT ESTIMATE OF THE ALTO XINGU SUB-BASIN, BRAZIL

Jocasta D. Ribeiro, Isabela M. S. Queiroz, Hans S. Santos
Department of Research and Extension, Production Engineering College,
Faculdade Salesiana Maria Auxiliadora, Macaé, Brazil

ABSTRACT

Aeromagnetic data were used to estimate the depth of the Alto Xingu Sub-Basin basement. This information may allow a better planning of new research activities in the region. The Alto Xingu Sub-Basin is a large area of approximately 200,000 km2 covered by closed forests in Brazil. The aeromagnetic data acquired allow the study of an underdeveloped region, located in a sedimentary basin, possible carrier of natural gas reservoirs and also shale gas. The Euler Deconvolution technique was applied after obtaining the magnetic anomaly in the region. Several structural index values and window sizes were tested. The Euler Deconvolution maps obtained allow to estimate the magnetic sources depth and to locate the regions of deeper sediment.

KEYWORDS: *Euler Deconvolution Application, Aeromagnetic Survey, Alto Xingu Sub-Basin, Oil and Gas Research*

I. INTRODUCTION

The aeromagnetic surveys are very useful for the mineral resources exploration. They allow sweeping large areas with low cost collecting important data that are used in geological research. The research arising from the acquisition of magnetic data of a sedimentary basin is one of the early stages of the search for new oil fields.

Among many techniques used in the magnetic data processing, the Euler Deconvolution enables to estimate the magnetic sources depth and to locate regions of deeper sediments. Thus, it is possible to locate the regions of greatest sediment depth. The natural gas production perspective motivated PETROBRAS to promote various geophysical surveys in the Alto Xingu Sub-Basin. So, it is entirely covered by aeromagnetic surveys such as those provided by the National Agency of Petroleum, Natural Gas and Biofuels (ANP). In this context, a network nearly 200,000 km^2 of treatable magnetic data were made available for research. By processing these data, we intend to identify faulting regions and to estimate sediments depth of the basin. This information is very useful for management of oil resources in the region.

Braga in paper [1], constructed a three-dimensional gravity modeling of the basement constrained by spectral estimates of depth to magnetic sources. Bahia in paper [2], updated the geological knowledge of the region and determined its tectonic domains using gravity and magnetic potential methods. Ribeiro & Santos in paper [3], determined the basin magnetic anomaly and located the areas with the greatest geological faulting events. There is still the necessity to confirm the regions with the greatest depths of sediments that are more attractive to promote new researches. Therefore, in this paper, Section 2 presents the characteristics of studied area as location, topography, geology, some results of previous researches and the data used in this work. Section 3 summarizes the theoretical basis of magnetometry and Euler Deconvolution that were the techniques used in this work. Section 4 describes the data processing and presents the results using maps. Section 5 summarizes the main results obtained and the conclusions of this paper.

II. STUDIED AREA CHARACTERISTICS

The Alto Xingu Sub-Basin is located in the eastern sector of the Parecis Basin (Figure 1) [4]. The region has many active petroleum systems and points of gas exudation as found by more than 800 meters along the Teles Pires River. In this region, six blocks were auctioned in the Tenth Round of Oil and Gas Bids [5].

Figure 1. Brazilian Paleozoic basins [4]

The terrain topographic map indicates that in most of the basin the altitudes range from 200 meters (blue portion of Figure 2) to 500 meters in the southern portion of the basin (pink part of Figure 2) [3].

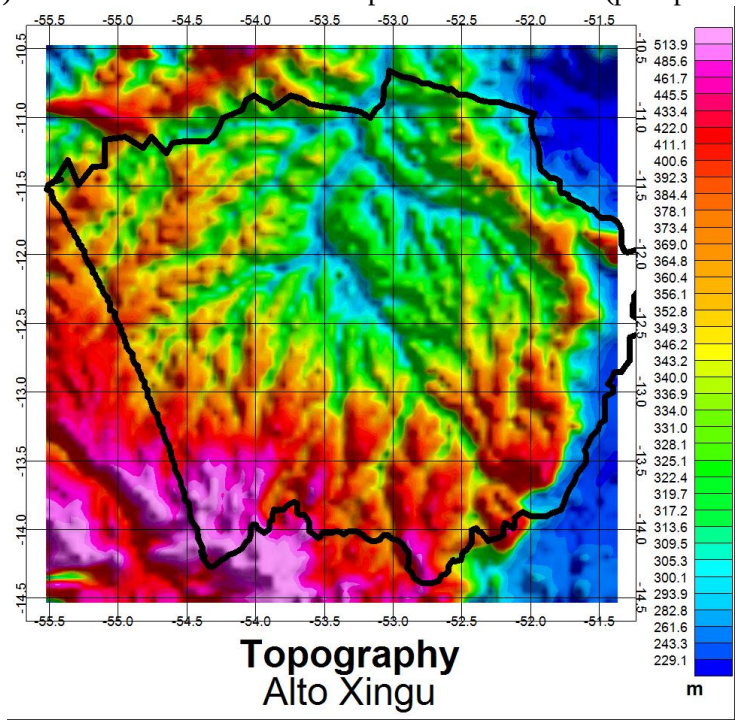

Figure 2. Alto Xingu Sub-Basin Topography [3]

The basin contains sediments of the Paleozoic, Mesozoic and Cenozoic, including Cretaceous volcanic rocks (Figure 3). Its base is the Amazonian Craton, comprising metamorphic, meta sedimentary and intrusive rocks.

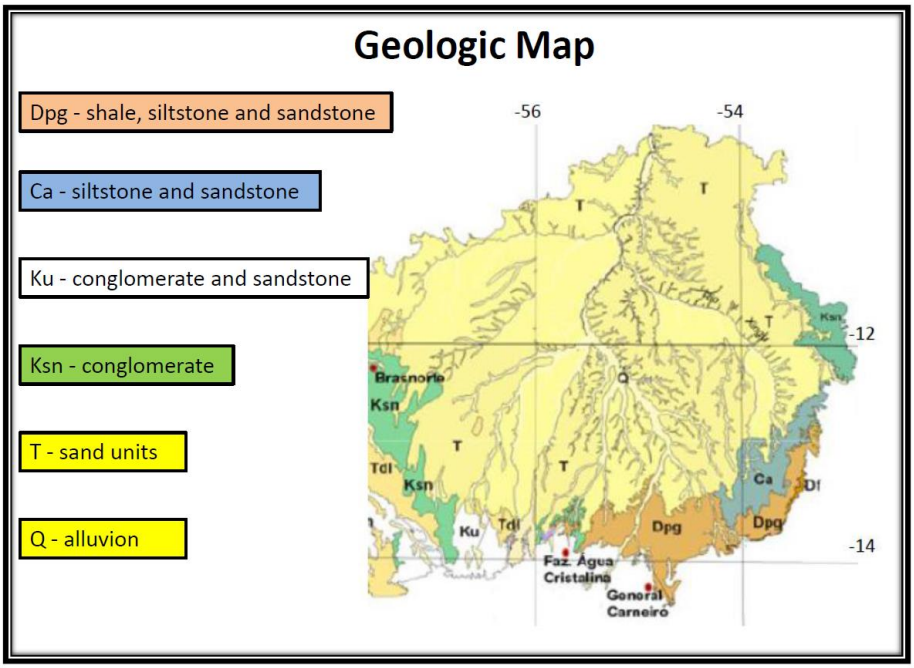

Figure 3. Alto Xingu Sub-Basin Geologic Map [2]

The region is separated from the Juruena Sub-Basin by the Serra Formosa Arc. It has the southern edge with the Paraná Basin. The Alto Xingu Sub-Basin tectonic areas are shown in Figure 4.

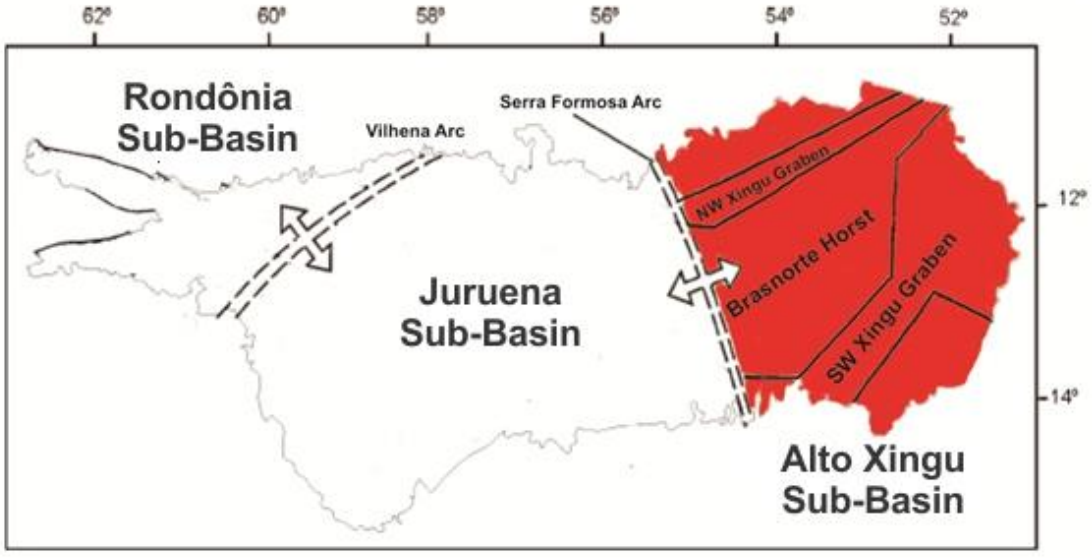

Figure 4. Tectonic Domain of the Alto Xingu Sub-Basin [2]

The basement topography in meters was obtained using an inversion technique based on continued down of the gravity field linked to the equivalent density layer principle (Figure 5) [1].

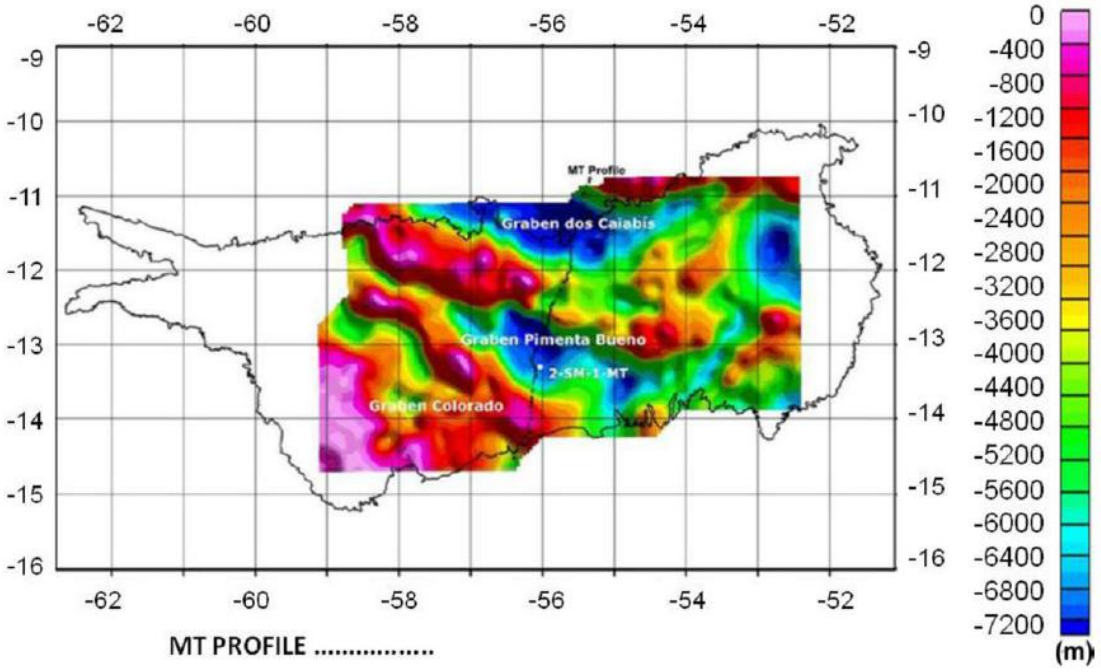

Figure 5. Gravity modeling of the Parecis Basin [1]

The data of two aeromagnetic surveys (Figure 6) with an altitude at 1,000 m, sampling interval of 50 m and control lines spaced at 18 km are available. The west block corresponds to a survey conducted by an Islander aircraft covering an area of 94,662 km^2 with flight lines spaced at 3 km. And the west block corresponds to a survey conducted by a Dehavilland aircraft covering an area of 101,850 km^2 with flight lines spaced at 6 km.

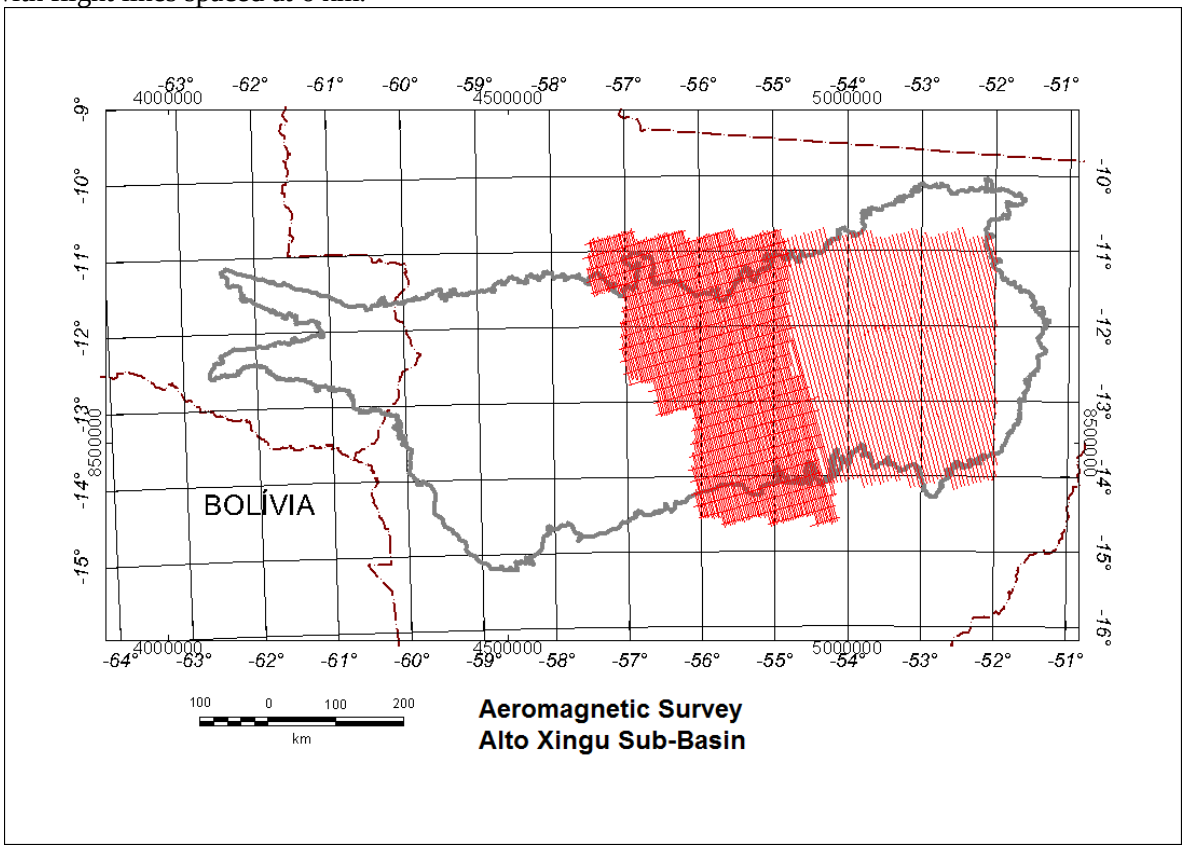

Figure 6. Aeromagnetic data available

III. METHODS

3.1. Magnetometry

When Earth's magnetic field measurement is made, the measured value is the superposition result of contributions that have different origins:

- The main field generated in the Earth's fluid core by a geodynamo mechanism.
- The crustal field generated by magnetized rocks in the Earth's crust.
- The external field produced by electric currents flowing in the ionosphere and the magnetosphere due to the interaction of electromagnetic radiation and the solar wind with the Earth's magnetic field [6].

The magnetic field is measured by a device called magnetometer. It measures a combined signal of the Main Field, External Field and Crustal Field. However, only the Crustal Field is important to mineral exploration. This field can be obtained by isolating and obtaining the Magnetic Anomaly. After the isolation of it, we can apply enhancement techniques that provide important subsoil information as the location of the faulting regions and the basement depth [7].

Thus, the magnetometry is performed through the following steps:

(1) Measuring the terrestrial magnetic field at predetermined points,

(2) Correction of measurements for knowing changes, and

(3) Comparing the field resulting value with the expected value at each measurement station. The field expected value is considered to be the International Geomagnetic Reference Field (IGRF).

The difference between observed and expected values is called magnetic anomaly [8].

The magnetometric process can be enhanced through the use of aircraft equipped with magnetometers. The aircraft can fly large areas acquiring a wide range of evenly spaced measurements. Generally, sedimentary rocks have lower magnetic susceptibility than the igneous and metamorphic rocks (Figure 7) [9].

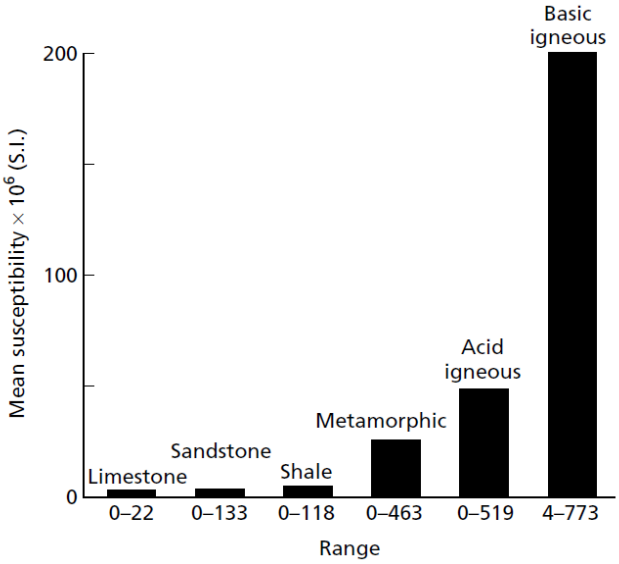

Figure 7. Magnetic susceptibilities of some rocks [9]

So, when the magnetic anomalies are observed in areas covered by sediments, they are usually formed by the crystalline basement (igneous or metamorphic), as well as intrusions. Dykes, sills, intrusions of igneous or metamorphic rocks and the crystalline basement rocks rich in magnetite ores are the most common causes of magnetic anomalies in sedimentary basins [9].

3.2. The Euler Deconvolution

The Euler Deconvolution technique allows estimating the magnetic sources depth from magnetic subsurface data. The technique was developed from studies done on interpretation of magnetic data on a large scale through aerial surveys. There is a combination of flexibility and simplicity in the algorithms used by the method.

The Euler Deconvolution uses the Euler's homogeneity equation to enable estimation of the position, depth and type of magnetic sources:

$$x\frac{\partial T}{\partial x}+y\frac{\partial T}{\partial y}+z\frac{\partial T}{\partial z}=NT \quad (1)$$

where T is the magnetic field and N is the homogeneity degree called structural index. This index depends on the geometry of the magnetic source that we want to explore (Table 1) [2].

Table 1: Structural Index table.

Structural Index (SI)	Source
0	Geological Contacts
0.5	Fautings regions
1	Dikes and Sills
2	Cylindrical Sources and Monopoles
3	Spherical Sources and Dipoles

In the data processing, it is always recommended to use all available structural indexes and then, analyze the index that provided the best results for the function groups. For each structural index chosen, we can estimate the geographical coordinates of the source that causes the anomaly by solving the Euler equation in a moving window of the total field measured at the point T_i (x, y, z) and with its derivatives in an overdetermined system:

$$\begin{bmatrix} \frac{\partial T_1}{\partial x} & \frac{\partial T_1}{\partial y} & \frac{\partial T_1}{\partial z} \\ \frac{\partial T_2}{\partial x} & \frac{\partial T_2}{\partial y} & \frac{\partial T_2}{\partial z} \\ \vdots & \vdots & \vdots \end{bmatrix} \begin{bmatrix} x-x_0 \\ y-y_0 \\ z-z_0 \end{bmatrix} = N \begin{bmatrix} T_1 \\ T_2 \\ \vdots \end{bmatrix} \quad (2)$$

After choosing the structural index, the dimensions of a moving window must be defined. This window runs across the mesh generating the set of solutions. The location of the sources will be seen as well-defined when there is a low dispersion of the solutions, so that different windows can provide solutions in similar positions (Figure 8) [10].

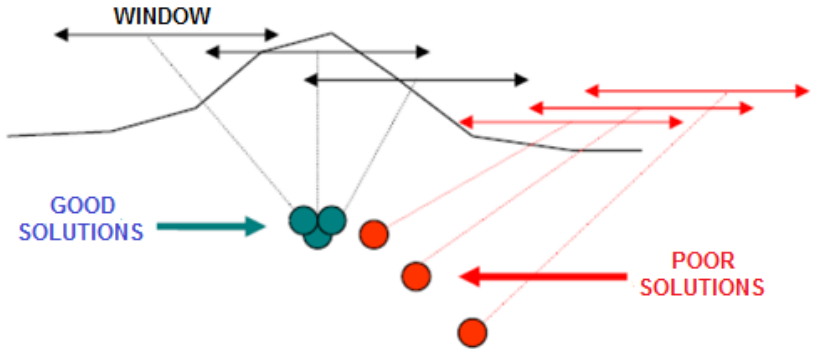

Figure 8. Quality of Euler deconvolution solutions [10]

Thus, the Euler Deconvolution is able to provide the position and depth of the various existing sources in the area surveyed, so independent of the main magnetic field direction and the source orientation. Thereby, it presents great results even in low latitude regions or areas with remnant magnetization. The main disadvantage of this method is that only a structural index can be used at a time, so the

technique is an unique source estimator. It limits the usage of the method in geologically complex areas [11].

IV. RESULTS

In the first stage of processing, the data inconsistencies as spikes and lacks were analyzed. Levelling and microlevelling techniques have been applied by using the Butterworth filter. Then, the raw data were given diurnal variation correction for the subtraction of the external magnetic field and the IGRF correction for subtraction of the main magnetic field. The result is the magnetic anomaly map made by a minimum curvature interpolation (Figure 9).

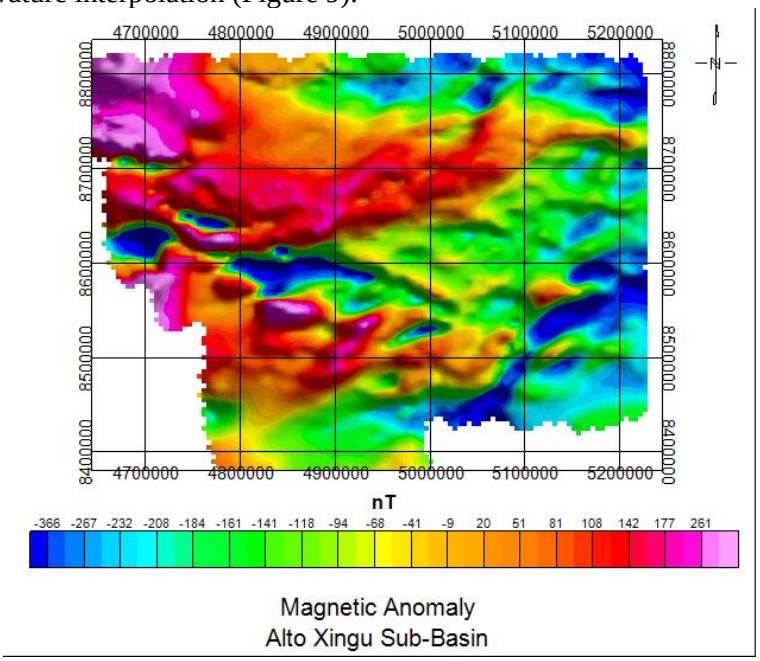

Figure 9. Magnetic Anomaly Map

This map reflects the crustal magnetic field in the region. It shows strong magnetic anomalies associated with the border regions between the Brasnorte Horst and adjacent grabens.
Then, the magnetic anomaly grid received a combination of vertical and horizontal derivatives filters:

$$A = \sqrt{\left(\frac{\partial T}{\partial x}\right)^2 + \left(\frac{\partial T}{\partial y}\right)^2 + \left(\frac{\partial T}{\partial z}\right)^2} \quad (3)$$

where T is potential field anomaly and $\left(\frac{\partial T}{\partial x}\right)$, $\left(\frac{\partial T}{\partial y}\right)$ and $\left(\frac{\partial T}{\partial z}\right)$ (horizontal derivative in x and y and vertical derivative in z). The result is the analytic signal map shown in the Figure 10.

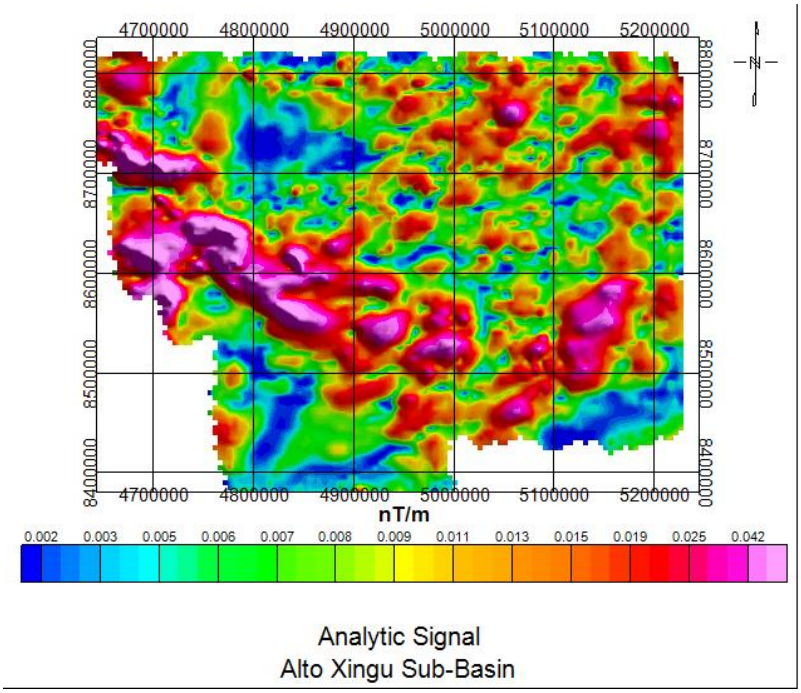

Figure 10. Analytic Signal Map

The analytical signal amplitude allows the location of the magnetic source without the incorporation of the permanent magnetization. The Euler Deconvolution technique was applied from the analytic signal in order to investigate the basement depth. Various values of tolerance, structural index (SI) and window sizes were tested for the Euler Deconvolution. The best results were obtained with 10% tolerance and 20 km windows. They allow mapping the major sources that are more interesting when we want to determine the basement depth from a sedimentary basin.

The Euler Deconvolution application with Structural Index SI = 0 (Figure 11) is able to map the geological contacts which are surfaces that separate rock units with different characteristics. The depths range from nearly 800 m to 6,400 m. However, most of the contacts identified were located at depths less than 2,000 m.

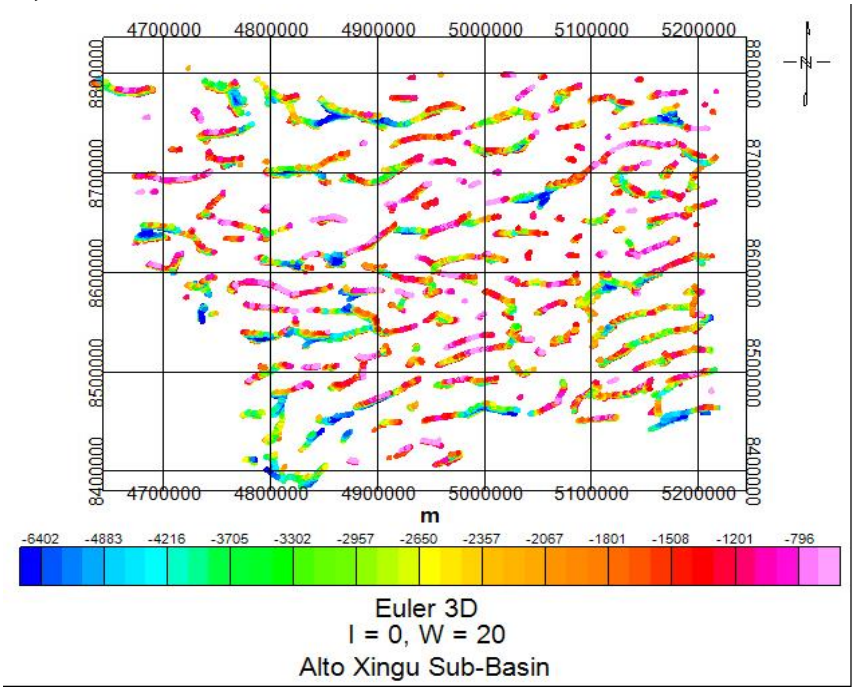

Figure 11. Euler Deconvolution Map with Structural index SI = 0

The Euler Deconvolution application with Structural Index SI = 0.5 (Figure 12) is able to map the basin faults as the separation regions between the grabens and horsts. The depths ranged nearly from 1,300 m to 7,500 m. The Pimenta Bueno Graben and the SW Xingu Graben were well located, in regions with large numbers of solutions in blue denoting depths around 7,000 m. The Brasnorte Horst was also well located at north of the Pimenta Bueno Graben with depths ranging from 1,300 m to 3,000 m, denoting the shallower region of the sedimentary basin. Thus, it was consistent with the gravity modeling map (Figure 5).

The Euler Deconvolution application with Structural Index SI = 1 (Figure 13) is able to map the regions with intrusion as dykes and sills. The depths ranged nearly from 1,700 m to 8,000 m. The Pimenta Bueno Graben and the SW Xingu Graben were well located, in regions with large numbers of solutions in blue denoting the greatest depths. The Brasnorte Horst was well located as the shallowest part of the basin in red.

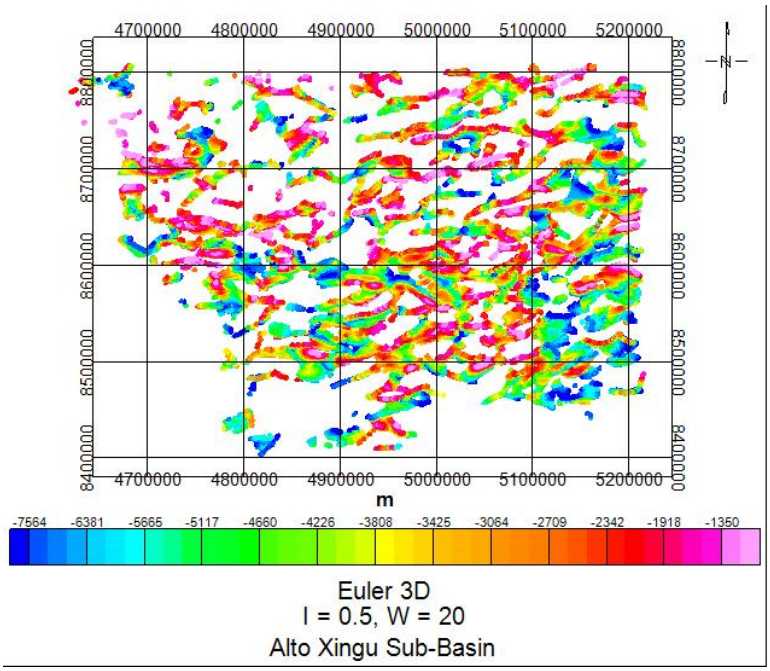

Figure 12. Euler Deconvolution Map with Structural index SI = 0.5

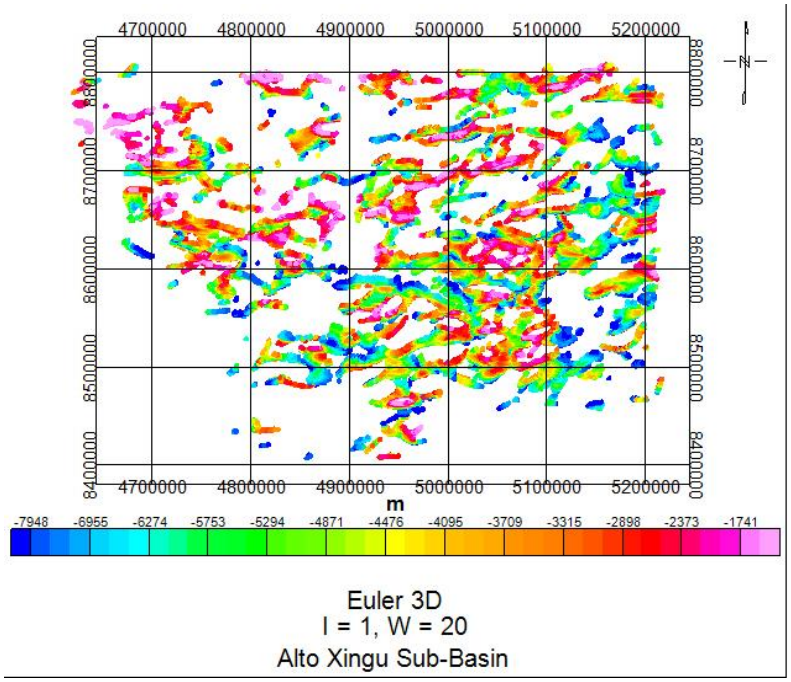

Figure 13. Euler Deconvolution Map with Structural index SI = 1.

The Euler Deconvolution application with Structural Index SI = 2 (Figure 14) is often used with lower window values with goal to mapping cylindrical sources as kimberlite chimneys that may be carrying diamonds regions. The use of Structural Index SI = 3 (Figure 15) is able to map spherical sources. The 2 and 3 index solution did not characterize the sedimentary basin structure. However, the few solutions found are compatible with the basement depth.

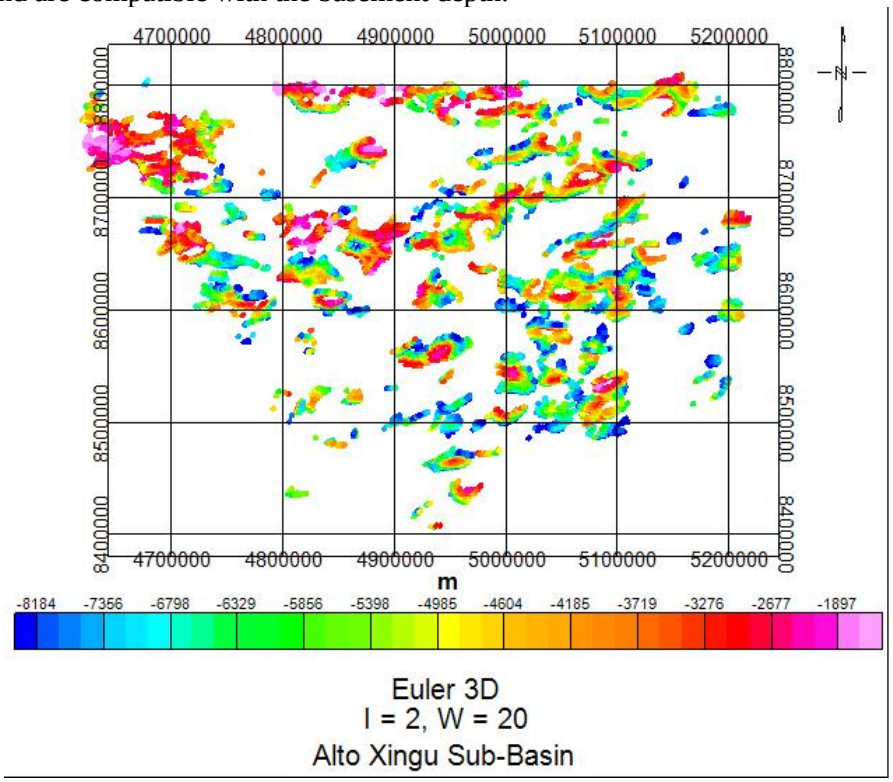

Figure 14. Euler Deconvolution Map with Structural index SI = 2

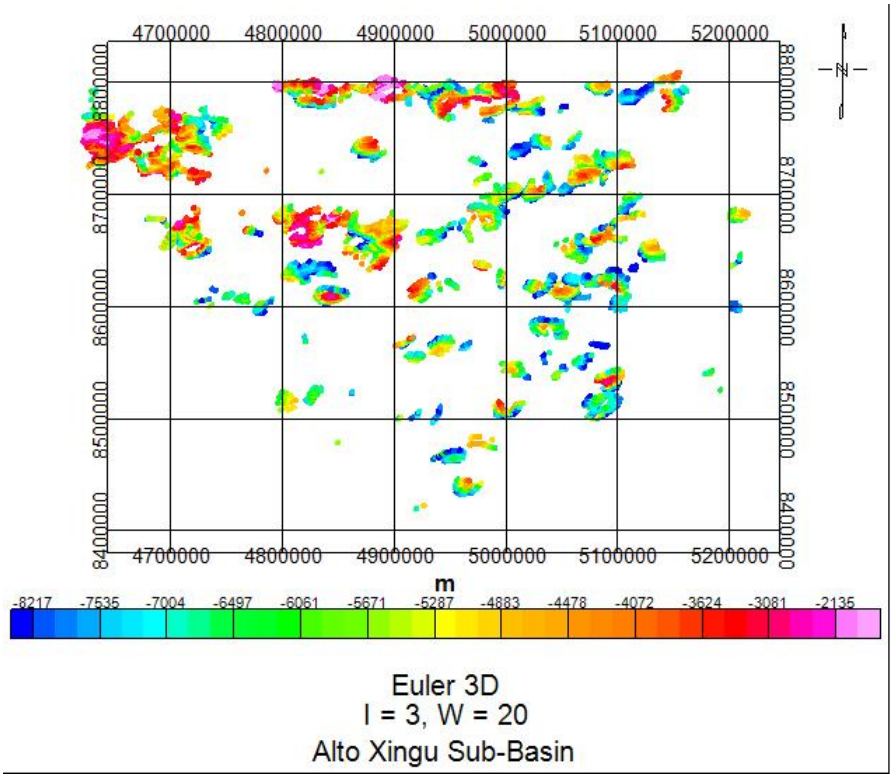

Figure 15. Euler Deconvolution Map with Structural index SI = 3

V. CONCLUSIONS

The Euler Deconvolution application in the Alto Xingu Sub-Basin allowed to estimating the depth of the basin sediments. The estimated depth ranged nearly from 6,500 m over to 8,000 m depending on the chosen Structural Index. These depth values were very close to the found value in the basin gravity modeling (Figure 5). The maps with 0 and 0.5 structural indexes allowed us to visualize the direction of the basin faulting with a predominance of guidelines on the northeast-southwest direction. However, the maps with 2 and 3 structural indexes did not allow to visualizing effectively the structure of the region. Soon, cylindrical and spherical sources are not very representative in the generation of magnetic anomaly. For future studies, a joint modeling procedure of gravity and magnetic data using link wells in the region is recommended.

ACKNOWLEDGEMENTS

The authors thank the reviewers for their valuable recommendations. In addition, the authors would like to express their thanks to the Research and Extension Coordinator Rodrigo S. Melo and the Engineering Production Coordinator André A. Manzela from Faculdade Salesiana Maria Auxiliadora for trusting and supporting the work.

REFERENCES

[1] Braga, Luiz Fernando Santana & Siqueira, Luiz Peixoto (1995) "Three-dimensional gravity modeling of the basement topography beneath Parecis Basin, Brazil, constrained by spectral estimates of depth to magnetic sources." 5th Latin American Petroleum Congress, Nova Friburgo, Brazil.
[2] Bahia, Ruy Benedito Calliari (2007), "Evolução Tectonossedimentar da Bacia dos Parecis." Contribuição às Ciências da Terra-Vol.18. Fundação Universidade Federal de Ouro Preto. Ouro Preto.
[3] Ribeiro, Jocasta & Santos, Hans Schmidt (2014), "Magnetometry Applied in the Alto Xingu Sub-Basin, Mato Grosso, Brazil." Journal of Earth Sciences and Geotechnical Engineering, vol. 4, no. 3, 1-18. Scienpress Ltd.
[4] Dardenne, Marcel Auguste; Alvarenga, Carlos José Souza; Oliveira, Claudinei Gouveia; Lenharo, Sarah Lais Rahal (2006), "Geologia e Metalogenia do Depósito de Cobre do Graben do Colorado, Fossa Tectônica de Rondônia, Brasil." Caracterização de Depósitos Minerais em Distritos Mineiros da Amazônia. Universidade de Brasília.
[5] Santos, Hans Schmidt & Flexor, Jean Marie, (2013) "Estudo da Bacia dos Parecis a partir da Integração de Dados Gravimétricos, Magnetométricos e Magnetotelúricos." São Paulo, UNESP, Geociências, v. 32, n.3, p.411-428.
[6] Lanza, Roberto & Meloni, Antonio (2006), "The Earth's Magnetism, An Introduction of Geologists". Springer. 2006.
[7] Blakely, Richard (1995), "Potential Theory in Gravity and Magnetic Applications." Cambridge University.
[8] Lowrie, William (2007) "Fundamentals of Geophysics". Swiss Federal Institute of Technology, Zürich. Cambridge University Press. Second Edition.
[9] Kearey, Philip; Brooks, Michael & Hill, Ian. (2002). "An Introduction to Geophysical Exploration." Third Edition. Blackwell Science Ltd.
[10] Silva, José Ribamar Silveira (2007), "Estudo do Levantamento Aerogeofísico do Estado do Rio de Janeiro na Região dos Lagos." Observatório Nacional, Rio de Janeiro.
[11] Guimarães, Suze Nei (2009) "Avanços recentes na determinação das estruturas geológicas em subsuperfície da Província Uranifera Lagoa Real (BA) a partir de dados aerogeofísicos." Observatório Nacional. Dissertação de Mestrado.

AUTHORS

Jocasta D. Ribeiro is a production engineering trainee working in oil exploration area of the Petrobras. She is an undergraduate in production engineering course with emphasis in marine facilities of the Faculdade Salesiana Maria Auxiliadora, Brazil.

Isabela M. S. Queiroz is an undergraduate in production engineering course with emphasis in marine facilities of the Faculdade Salesiana Maria Auxiliadora, Brazil.

Hans S. Santos is a Ph.D. in geophysics by the Observatório Nacional, Brazil. He is currently professor of the department of research and extension. He is supervisor of undergraduate works of the Faculdade Salesiana Maria Auxiliadora, Brazil.